Available online at www.sciencedirect.com
SCIENCE DIRECT®
Journal of Power Sources 143 (2005) 173–178
JOURNAL OF POWER SOURCES
www.elsevier.com/locate/jpowsour

Short communication

An approximate closed form solution for pressure and velocity distribution in the cathode chamber of a PEM fuel cell

Vamsi K. Maddirala, Venkat R. Subramanian*

Department of Chemical Engineering, Tennessee Technological University, Cookeville, TN 38505, USA

Received 8 November 2004; accepted 28 November 2004
Available online 10 February 2005

Abstract

In this paper, an approximate technique is used to obtain pressure and velocity distribution in the cathode chamber of PEM fuel cells. The technique is based on polynomial profile approximation. The technique predicts two dimensional pressure and velocity distribution in closed form as a function of independent variables. The approximate solution developed compares reasonably with the rigorous numerical solution.

Keywords: PEM fuel cell; Cathode chamber; Pressure and velocity distributions

1. Introduction

Fuel cells are devices that convert chemical energy directly into electrical energy. Fuel cells are believed to be a most promising power source for a wide range of applications by virtue of their high-energy efficiency, pollution free characteristics, compactness in design and operation. In the last decade significant improvement has been made in the design of PEM fuel cells.

Models for PEM fuel cells have features both common and different from models for secondary batteries. Because of recent interest in PEM fuel cells, researchers from various disciplines have started using different kind of models for PEM fuel cells according to their convenience/objectives/understanding [1–15]. Recently new models based on thermodynamics related equations have been developed to predict the performance of PEM fuel cells [28]. In order to accurately predict the performance of PEM fuel cells one has to solve different dependent variables including pressure, concentration (or mole fraction), electrolyte potential, temperature etc [29,30]. Models varying from 1D–3D, one region to 3 or 5 regions have been used in the literature [16–31]. Even for predicting two-dimensional pressure or velocity distribution accurately, only numerical solution has been used and reported in the literature.

Most of the model equations for PEM fuel cells are non-linear. However, the pressure distribution for oxygen inside the cathode chamber (Fig. 1) can be sufficiently described using the Laplace's equation [25]. Though the governing equation is linear (Laplace's equation), researchers haven't used analytical solution for pressure as the boundary condition at the top ($y = H$ in Fig. 1) has three different boundary conditions depending on the value for x [25,26]. In this paper, we arrive at approximate solutions for pressure and velocity distributions [32,34,35]. These approximate solutions will be fed into the non-linear convective-diffusion equation for concentration distribution in a later publication to arrive at analytical/efficient solution for two-dimensional concentration profiles for oxygen inside the cathode chamber shown in Fig. 1. The approximate model developed is compared with a rigorous numerical solution to analyze the accuracy of approximation.

1.1. Approximate models for pressure and velocity distributions

The cathode chamber shown in the Fig. 1 is modeled in this paper. The following assumptions are made:

* Corresponding author. Tel.: +1 931 372 3494; fax: +1 931 372 6352.
E-mail address: vsubramanian@tntech.edu (V.R. Subramanian).

0378-7753/$ – see front matter © 2005 Elsevier B.V. All rights reserved.
doi:10.1016/j.jpowsour.2004.11.059

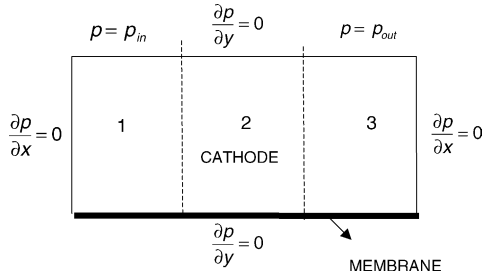

Fig. 1. Schematic of the cathode chamber modeled.

- Water exists only in the vapor form and the effects of pore plugging are neglected [42,43].
- The fuel cell is isothermal.
- Darcy's law is valid.
- Fluid is incompressible.
- Temperature does not affect pressure.
- The electrode layer is assumed to be homogeneous with uniform physical properties.
- Transport of the reactants in the electrode layer is neglected.

The governing equation for the pressure is given by Laplace's Eq. [25]

$$\left(\frac{\partial^2}{\partial x^2}p(x,y)\right)+\left(\frac{\partial^2}{\partial y^2}p(x,y)\right)=0 \tag{1}$$

The boundary conditions are summarized as follows,

$$\text{At } X=0, \quad \frac{\partial p}{\partial x}=0 \tag{2}$$

$$\text{At } X=L, \quad \frac{\partial p}{\partial x}=0 \tag{3}$$

$$\text{At the membrane } (y=0), \quad \frac{\partial p}{\partial y}=0 \qquad (0\le x\le L) \tag{4}$$

$$\text{At the inlet}, \quad p=p_{\text{in}} \qquad (y=H \text{ and } 0\le x\le L_1) \tag{5}$$

$$\text{At the current collector}, \quad \frac{\partial p}{\partial y}=0 \qquad (y=H \text{ and } L_1\le x\le L_2) \tag{6}$$

$$\text{At the outlet}, \quad p=p_{\text{out}} \quad (y=H \text{ and } L_2\le x\le L) \tag{7}$$

where, p_{in} is the inlet pressure and p_{out} is the outlet pressure. The following dimensionless variables are introduced,

$$P=\frac{p-p_{\text{out}}}{p_{\text{in}}-p_{\text{out}}}, \qquad Y=\frac{y}{H}, \qquad X=\frac{x}{L} \tag{8}$$

The governing equation and boundary conditions in dimensionless form are,

$$\varepsilon^2\left(\frac{\partial^2}{\partial X^2}P(X,Y)\right)+\left(\frac{\partial^2}{\partial Y^2}P(X,Y)\right)=0 \tag{9}$$

where $\varepsilon = H/L$ is the aspect ratio. The dimensionless boundary conditions are given by,

$$\text{At } X=0, \quad \frac{\partial P}{\partial X}=0 \qquad 0\le Y\le 1 \tag{10}$$

$$\text{At } X=1, \quad \frac{\partial P}{\partial X}=0 \qquad 0\le Y\le 1 \tag{11}$$

$$\text{At the membrane } (Y=0), \quad \frac{\partial P}{\partial Y}=0 \qquad (0\le X\le 1) \tag{12}$$

$$\text{At the inlet} \quad P=1 \qquad \left(Y=1 \text{ and } 0\le X\le \frac{L_1}{L}\right) \tag{13}$$

$$\text{At the current collector} \quad \frac{\partial P}{\partial Y}=0 \qquad \left(Y=1 \text{ and } \frac{L_1}{L}\le X\le \frac{L_2}{L}\right) \tag{14}$$

$$\text{At the outlet} \quad P=0 \qquad \left(Y=1 \text{ and } \frac{L_2}{L}\le X\le 1\right) \tag{15}$$

Next, a polynomial approximation is made for pressure in each region [11,12]. For region 1 pressure is taken as,

$$P_1(X,Y)=a_0(X)+a_1(X)Y^2 \tag{16}$$

$$\text{For region 2}, \quad P_2(X,Y)=b_0(X)+b_1(X)Y^2 \tag{17}$$

$$\text{and for region 3}, \quad P_3(X,Y)=c_0(X)+c_1(X)Y^2 \tag{18}$$

Note that the term 'Y' is left in Eqs. (16)–(18) to satisfy the boundary condition at $Y=0$ (Eq. (12)). Next, the functions $a_0(X)$, $a_1(X)$, $b_0(X)$, $b_1(X)$, $c_0(X)$ and $c_1(X)$ are found.The volume averaged equation for pressure in the first region ($P_1\text{ave}(X)$) is given by integrating the approximation equation for $P_1(X,Y)$ in y direction from 0 to 1.

$$\int_0^1 P_1(X,Y)\,\mathrm{d}y = P_1\text{ave}(X)=a_0(X)+\frac{1}{3}a_1(X) \tag{19}$$

By applying the boundary condition at $Y=1$ in the first region i.e., substituting Eq. (13) in Eq. (16) we get:

$$a_0(X)+a_1(X)-1=0 \tag{20}$$

Eqs. (17) and (18) are solved to get

$$\begin{aligned} a_0(X)&=\frac{3}{2}P_1\text{ave}(X)-\frac{1}{2}\\ a_1(X)&=-\frac{3}{2}P_1\text{ave}(X)+\frac{3}{2}\end{aligned} \tag{21}$$

By substituting Eq. (21) in Eq. (16) we get,

$$P_1(X,Y) = \frac{3}{2}P_1\text{ave}(X) - \frac{1}{2} + \left(-\frac{3}{2}P_1\text{ave}(X) + \frac{3}{2}\right)Y^2 \tag{22}$$

Next, the approximation equation (Eq. (22)) is substituted in the governing equation (Eq. (8)) and integrated in Y from 0 to 1 to get

$$\varepsilon^2\left(\frac{d^2}{dX^2}P_1\text{ave}(X)\right) - 3P_1\text{ave}(X) + 3 = 0 \tag{23}$$

Similarly the governing equations for volume averaged pressures in regions 2 and 3 are obtained after similar steps as:

$$\varepsilon^2\left(\frac{d^2}{dX^2}P_2\text{ave}(X)\right) = 0 \tag{24}$$

$$\varepsilon^2\left(\frac{d^2}{dX^2}P_3\text{ave}(X)\right) - 3\,P_3\text{ave}(X) = 0 \tag{25}$$

Note that a single partial differential equation (Eq. (9)) is converted to three second order ordinary differential equations (Eqs. (23), (24), and (25)). We need six boundary conditions to solve this system of boundary value problems. We get two boundary conditions by volume averaging the boundary conditions at $X = 0$ and $X = 1$ (Eqs. (10) and (11)).

$$\frac{dP_1\text{ave}}{dX} = 0 \text{ at } X = 0 \tag{26}$$

$$\frac{dP_3\text{ave}}{dX} = 0 \text{ at } X = 1 \tag{27}$$

Next, the pressure and its gradient should be continuous at $X = (1/4)$ and at $X = (3/4)$. By volume averaging the continuity of pressure and its gradient we obtain,

$$\text{At } X = \tfrac{1}{4}, \qquad P_1\text{ave}(X) = P_2\text{ave}(X) \tag{28}$$

$$\frac{dP_1\text{ave}(X)}{dX} = \frac{dP_2\text{ave}(X)}{dX} \tag{29}$$

$$\text{and at } X = \tfrac{3}{4}, \qquad P_2\text{ave}(X) = P_3\text{ave}(X) \tag{30}$$

$$\frac{dP_2\text{ave}(X)}{dX} = \frac{dP_3\text{ave}(X)}{dX} \tag{31}$$

Solving the governing equations (Eqs. (23), (24) and (25)) using the six boundary conditions given in the Eqs. (26), (27), (28), (29), (30) and (31) we get,

$$P_1\text{ave}(X) = 1 - \frac{2\varepsilon\,\cos h(\sqrt{3}X/\varepsilon)}{4\,\cos h(\sqrt{3}/4\varepsilon) + \sin h(\sqrt{3}/4\varepsilon)\sqrt{3}} \tag{32}$$

$$P_2\text{ave}(X) = 1 + \frac{2\,\sin h(\sqrt{3}/4\varepsilon)\sqrt{3}X}{4\,\cos h(\sqrt{3}/4\varepsilon) + \sin h(\sqrt{3}/4\varepsilon)\sqrt{3}} + \frac{1}{2}\frac{\sin h(\sqrt{3}/4\varepsilon)\sqrt{3}}{4\,\cos h(\sqrt{3}/4\varepsilon) + \sin h(\sqrt{3}/4\varepsilon)\sqrt{3}} - \frac{2\,\cos h(\sqrt{3}/4\varepsilon)}{4\,\cos h(\sqrt{3}/4\varepsilon) + \sin h(\sqrt{3}/4\varepsilon)\sqrt{3}} \tag{33}$$

$$P_3\text{ave}(X) = \frac{2\varepsilon\,\cos h(\sqrt{3}(1-X)/\varepsilon)}{4\cos h(\sqrt{3}/4\varepsilon) + \sin h(\sqrt{3}/4\varepsilon)\sqrt{3}} \tag{34}$$

By substituting the above expressions in Eqs. (16), (17), (18) and (22) we get

$$P_1(X,Y) = 1 - \left[\frac{3\varepsilon\,\cos h(\sqrt{3}X/\varepsilon)}{4\,\cos h(\sqrt{3}/4\varepsilon) + \sin h(\sqrt{3}/4\varepsilon)\sqrt{3}}\right] + \left[\frac{3\varepsilon\,\cos h(\sqrt{3}X/\varepsilon)}{4\,\cos h(\sqrt{3}/4\varepsilon) + \sin h(\sqrt{3}/4\varepsilon)\sqrt{3}}\right]Y^2 \tag{35}$$

$$P_2(X,Y) = 1 - \left[\frac{2\,\sin\,h(\sqrt{3}/4\varepsilon)\sqrt{3}}{4\,\cos\,h(\sqrt{3}/4\varepsilon) + \sin\,h(\sqrt{3}/4\varepsilon)\sqrt{3}}\right]X + \frac{1}{2}\frac{\sin\,h(\sqrt{3}/4\varepsilon)\sqrt{3}}{4\,\cos\,h(\sqrt{3}/4\varepsilon) + \sin\,h(\sqrt{3}/4\varepsilon)\sqrt{3}} - \frac{2\varepsilon\,\cos\,h(\sqrt{3}/4\varepsilon)}{4\,\cos\,h(\sqrt{3}/4\varepsilon) + \sin\,h(\sqrt{3}/4\varepsilon)\sqrt{3}} \tag{36}$$

$$P_3(X,Y) = \left[\frac{3\varepsilon\,\cos h(\sqrt{3}(1-X)/\varepsilon)}{4\,\cos h(\sqrt{3}/4\varepsilon) + \sin h(\sqrt{3}/4\varepsilon)\sqrt{3}}\right] - \left[\frac{3\varepsilon\cos h(\sqrt{3}X/\varepsilon)}{4\cos h(\sqrt{3}/4\varepsilon) + \sin h(\sqrt{3}/4\varepsilon)\sqrt{3}}\right]Y^2 \tag{37}$$

Note that a closed form solution for pressure is obtained in terms of aspect ratio ε. The dimensionless velocity components U and V in x and y directions respectively are calculated using the following equations

$$U = -\frac{\partial P}{\partial X} \tag{38}$$

$$V = -\frac{\partial P}{\partial Y} \tag{39}$$

2. Results and discussion

Parameters (L_1, L_2, L and ε) in the model are taken from literature [25] and are listed in Table 1. Fig. 2 shows the distribution for dimensionless pressure predicted using the

Table 1
Modeling parameters in the electrode

Cathode width, L	0.18 cm
Cathode height, H	0.02 cm
Length of region 1, L_1	$L/4$
Length of region 2, L_2	$L/2$
Length of region 3, L_3	$L/4$

approximate model developed. From Fig. 2 we observe that pressure varies linearly in the cathode chamber between the current collector and the membrane.

In the following figures, rigorous numerical solution obtained by solving Eq. (9) with Eqs. (10)–(14) using FEMLAB [32] is used for comparison.

Fig. 3, shows the profiles for dimensionless pressure at the boundary $X = 0$. The approximate solution developed in this paper is compared with a rigorous 2D numerical solution

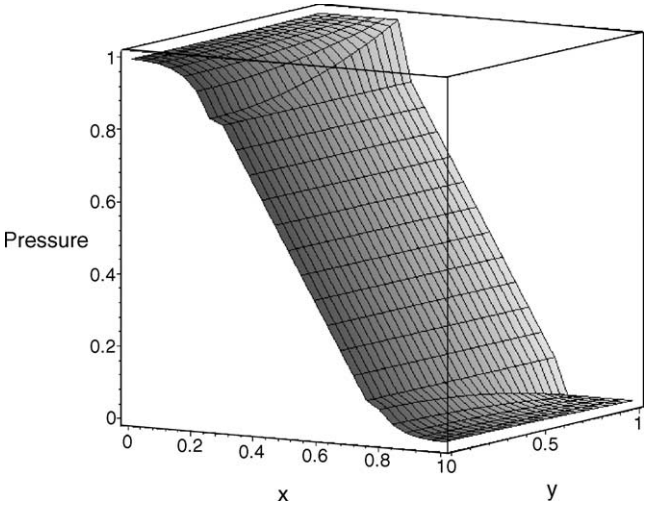

Fig. 2. Profile for dimensionless pressure distribution in the cathode of a PEM Fuel cell.

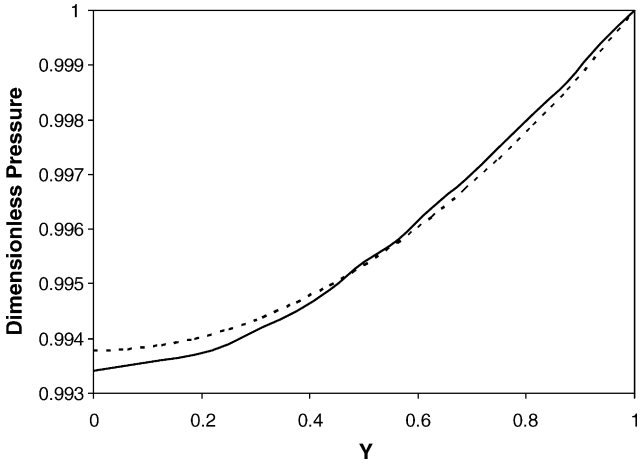

Fig. 3. Dimensionless pressure distribution at $X = 0$. Dotted line corresponds to the approximate model developed. Solid line corresponds to the rigorous numerical solution.

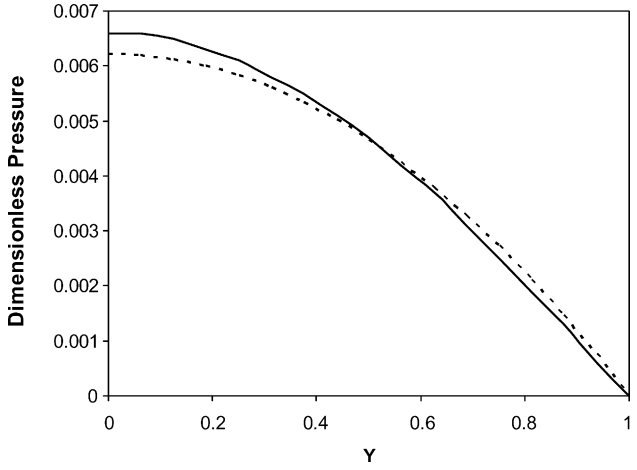

Fig. 4. Dimensionless pressure distribution at $X = 1$. Dotted line corresponds to the approximate model developed. Solid line corresponds to the rigorous numerical solution.

obtained using FEMLAB, a finite element software [32]. Both the curves started at 0.993 and ended at 1.

Fig. 4 shows the profile for dimensionless pressure at the boundary $X = 1$. In this case also there is a minor difference in the magnitude (around 0.001).

Fig. 5 shows the profile for dimensionless pressure at the boundary $Y = 0$. At this boundary cathode channel and membrane come into contact. Knowledge of gas pressure at this interface is important because, oxygen passes through cathode gas channel to the cathode catalyst layer where the electrochemical reaction takes place. The curves using numerical solution and the approximate model developed matches accurately excepting that there is slight bump in the curve obtained using maple at $X = 3/4$, this could be because of the reason that at the interface between second and third regions i.e., at $X = 3/4$, average pressures and their differentials are equated instead of equating pressures at values of X.

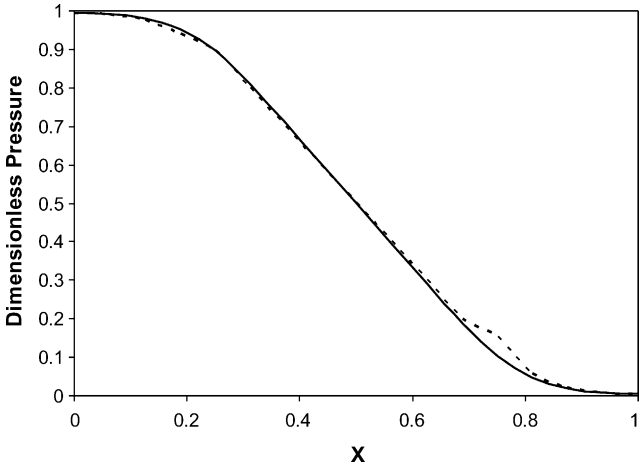

Fig. 5. Dimensionless pressure distribution at the membrane interface ($Y = 0$). Dotted line corresponds to the approximate model developed. Solid line corresponds to the rigorous numerical solution.

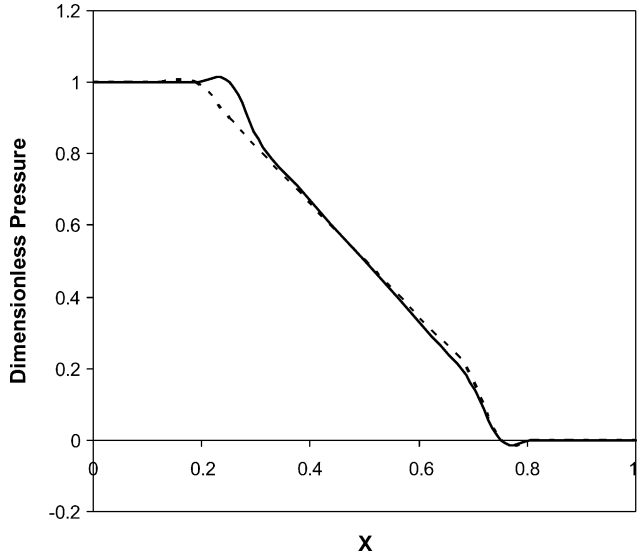

Fig. 6. Dimensionless pressure distribution at $Y = 1$. Dotted line corresponds to the approximate model developed. Solid line corresponds to the rigorous numerical solution.

Fig. 6 shows the profile for dimensionless pressure at the boundary $Y = 1$. Both the curves using FEMLAB and the approximate model developed matches well in this case, excepting at the interface between first and second regions i.e., at $X = 1/4$. The reason for this anomaly could be same as mentioned in the Fig. 5.

Figs. 7 and 8 show the comparison of vertical components of dimensionless velocity (V). The approximate model developed predicts the behavior reasonably well.

Fig. 9 shows the comparison of profiles for X component of dimensionless velocity U at $Y = 0$. The approximate model developed fails in capturing the behavior, especially at the interfaces at $X = 1/4$ and $X = 3/4$. To improve the accuracy one

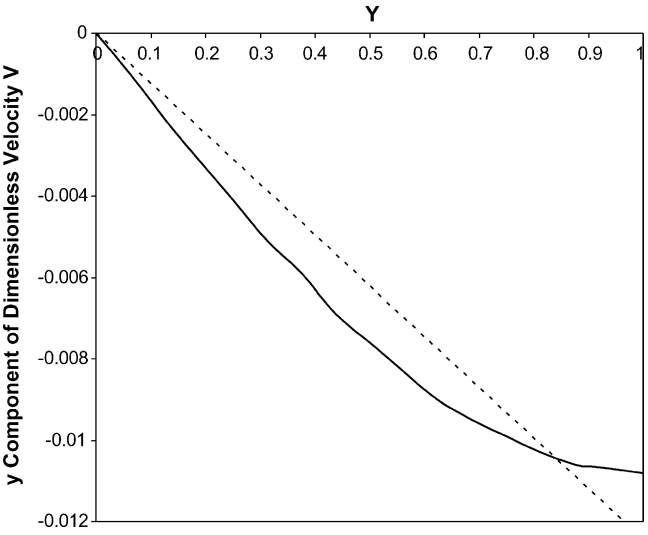

Fig. 7. Comparison of y component of dimensionless velocity (V) distribution at $X = 0$ and Y from 0 to 1. Dotted line corresponds to the approximate model developed. Solid line corresponds to the rigorous numerical solution.

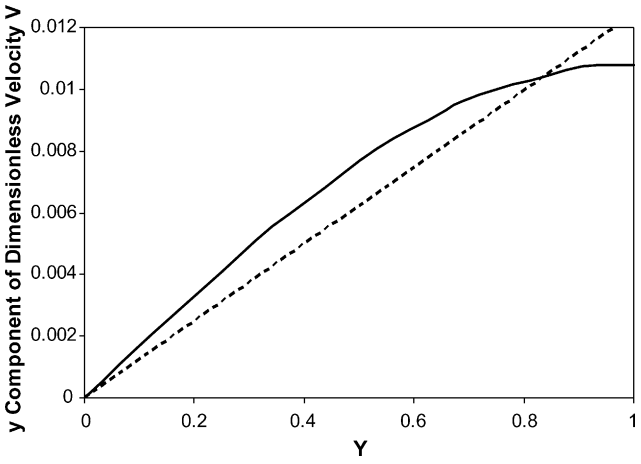

Fig. 8. Comparison of y component of dimensionless velocity (V) distribution at $X = 1$ and Y from 0 to 1. Dotted line corresponds to the approximate model developed. Solid line corresponds to the rigorous numerical solution.

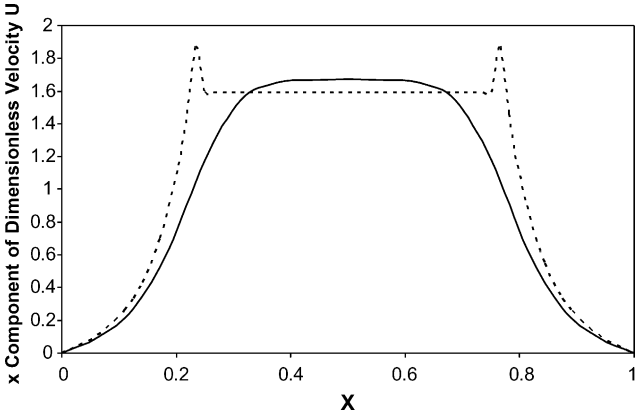

Fig. 9. Comparison of x component of dimensionless velocity (U) distribution at $Y = 0$. Dotted line corresponds to the approximate model developed. Solid line corresponds to the rigorous numerical solution.

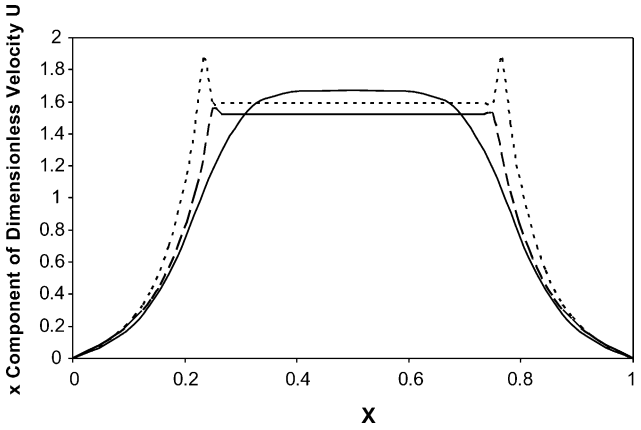

Fig. 10. Comparison of x component of dimensionless velocity (U) distribution at $Y = 0$. Dotted line corresponds to the approximate model developed. Solid line corresponds to the rigorous numerical solution. Dashed line corresponds to the improved approximate model.

can add more number of terms in the polynomial approximation (Eqs. (16) to (18)). Alternately we found that if we define

$$P_1\text{ave}(X) = \int_0^1 f(y)P_1(x, y)\mathrm{d}y$$

and redo the calculations, we obtain better results as shown in Fig. 10. We are currently working on optimizing a function $f(y)$ which can be used to obtain

$$P_1\text{ave}(X) = \int_0^1 f(y)P_1(x, y)\mathrm{d}y$$

we plan to publish this later.

3. Conclusions

In this paper, an approximate technique was used to obtain closed form solution for pressure and velocity distributions [32–41] as a function of system parameter, the aspect ratio ε. The approximate model predicts the behavior reasonably well.

For modeling PEM fuel cells in hybrid environment one has to simulate models for PEM fuel cells in series/parallel combination with models for batteries and other electrical components. This paper is our first step towards simplifying PEM fuel cell models for hybrid applications. In our future publications, we plan to use the approximate model developed for pressure and velocity distribution to solve the convection – diffusion equation [19,20,40,41] for oxygen concentration distribution in closed-form efficiently.

Acknowledgements

We would like to acknowledge the Center of Electric Power (CEP) and the Chemical Engineering Department at Tennessee Technological University for providing research and teaching assistantship to Vamsi K. Maddirala.

References

[1] N. Wakao, S. Kaguei, Heat and Mass transfer in Packed Beds, Gordon & Breach, New York, USA, 1982.
[2] D. Do, R. Rice, AIChE J. 32 (1986) 149.
[3] J.H. Hills, Chem. Eng. Sci. 11 (1986) 2779.
[4] D. Do, P.L.J. Mayfield, AIChE J. 33 (1987) 1397.
[5] T. Tomida, B.J. McCoy, AIChE J. 33 (1987) 1908.
[6] D. Do, T.V. Nguyen, Chem. Eng. Commun. 72 (1988) 171.
[7] M.A. Budzianowski, R.T. Yang, Chem. Eng. Sci. 44 (1989) 2683.
[8] D.H. Kim, AIChE J. 35 (1989) 343.
[9] M. Goto, J.M. Smith, B.J. McCoy, Chem. Eng. Sci. 45 (1990) 443.
[10] C.C. Lai, C.S. Tan, AIChE J. 37 (1991) 461.
[11] M. Goto, T. Hirose, Chem. Eng. Sci. 48 (1993) 443.
[12] C. Yao, C. Tien, Chem. Eng. Sci. 48 (1993) 187.
[13] R. Zhang, J.A. Ritter, Chem. Eng. Sci. 52 (1997) 3161.
[14] G. Carta, A. Cincotti, Chem. Eng. Sci. 53 (1998) 3483.
[15] G.G. Botte, R. Zhang, J.A. Ritter, Chem. Eng. Sci. 53 (1998) 4135.
[16] T.V. Nguyen, R.E. White, J. Electrochem. Soc. 140 (1993) 2178.
[17] T.E. Springer, T.A. Zawodzinski, S. Gottesfield, J. Electrochem. Soc. 138 (8) (1991).
[18] T.F. Fuller, J. Newman, J. Electrochem. Soc. 140 (1993) 1218–1225.
[19] T.V. Nguyen, R.E. White, J. Electrochem. Soc. 140 (1993) 2178–2186.
[20] V. Gurau, H. Liu, S. Kakac, AIChE J. 44 (11) (1998).
[21] K. Dannenberg, P. Ekdunge, G. Lindbergh, J. Appl. Electrochem. 30 (2000).
[22] G.J.M. Janssen, J. Appl. Electrochem. 148 (12.) (2001).
[23] S. Um, C.Y. Wang, K.S. Chen, J. Appl. Electrochem. 147 (12) (2000).
[24] H.K. Hsuen, J. Power Sources 123 (2000).
[25] A. Kazim, H.T. Liu, P. Forges, J. Appl. Electrochem. (1999) 1409–1416.
[26] W. He, J.S. Yi, T.V. Nguyen, AIChE J. 46 (10) (2000).
[27] T.V. Nguyen, J. Electrochem. Soc. 143 (1996) L103.
[28] M.L. Perry, J. Newman, E.J. Cairns, J. Electrochem. Soc. 145 (1) (1998) 5.
[29] K.E. Thomas, J. Newman, J. Electrochem. Soc. 150 (2) (2003) A176–A192.
[30] G. Murgia, L. Pisani, M. Valentini, B.D. Aguanno, J. Electrochem. Soc. 149 (1) (2002) A31–A38.
[31] D.M. Bernardi, M.W. Verbrugge, J. Electrochem. Soc. 139 (9) (1992).
[32] V.R. Subramanian, J.A. Ritter, R.E. White, J. Electrochem. Soc. 148 (11) (2001) E444–E449.
[33] J.S. Newman, Electrochemical Systems, Prentice Hall, Englewood Cliffs, NJ, 1991.
[34] C.H. Liaw, J.S.P. Wang, R.H. Greenkorn, K.C. Chao, AIChE J. 54 (1979) 376.
[35] G.G. Botte, R. Zhang, J.A. Ritter, Adsorption 5 (1999) 375.
[36] M. Doyle, T.F. Fuller, J. Newman, J. Electrochem. Soc. 140 (1993) 1526.
[37] W.B. Gu, C.Y. Wang, B.Y. Liaw, J. Electrochem. Soc. 145 (1998) 3407.
[38] W.B. Gu, C.Y. Wang, B.Y. Liaw, J. Electrochem. Soc. 145 (1998) 3418.
[39] T.E. Springer, T.A. Zawodzinski, S. Gottesfield, J. Electrochem. Soc. 138 (1991) 2334–2342.
[40] V. Gurau, H. Liu, S. Kakac, AIChE J. 44 (1998) 2410.
[41] J.T. Wang, R.F. Savinell, Electrochem. Acta 37 (1992) 2737.
[42] T. Thampan, S. Malhotra, H. Tang, D. Ravindra, J. Electrochem. Soc. 147 (9) (2000) 3242–3250.
[43] S Um, C.Y. Wang, K.S. Chen, J. Electrochem. Soc. 147 (12) (2000) 4485–4493.